Canadian Science Publishing

ARTICLE

Simulating the impacts of land reclamation and de-reclamation on the morphodynamics of tidal networks[1]

Lei Chen, Zeng Zhou, Fan Xu, Mirian Jimenez, Jianfeng Tao, and Changkuan Zhang

Abstract: The morphodynamic responses of tidal networks to anthropogenic reclamation and de-reclamation projects are investigated through a three-stage numerical simulation. In the first stage, the natural development of tidal networks is modelled in an open coast without any anthropogenic interventions. At the beginning of the second stage, parts of the computational domain are enclosed by sea dikes, which represents the implementation of the reclamation project. These sea dikes are removed or opened in the third stage to simulate the recovery of the tidal networks after de-reclamation. Each stage was set to last 100 years. The model results indicate that land reclamation can lead to three effects on tidal network morphology: (*i*) completely terminating the development of channels inside the projected area, (*ii*) hindering the development of the channel network in front of the dikes, and (*iii*) turning the channel direction near the corners of the dikes. When removing all the sea dikes, the previously reclaimed areas are quickly occupied by tidal networks. However, the morphology cannot be fully restored to its original natural state, although the entire reclaimed areas are returned. The effects of opening breaches are relatively slow, and tree-like network structures are formed inside the reclaimed areas.

Key words: land reclamation, de-reclamation, tidal networks, morphodynamic modeling.

1. Introduction

Land reclamation has been one of the major anthropogenic activities in coastal areas for the demand of land resources (Portnoy and Giblin 1997). Large-scale land reclamation projects have pronouncedly changed the coastline worldwide and have caused morphological and ecological problems because of the lack of effective management (Lotze et al. 2006), such as the sharp loss of intertidal flats and associated wetland ecosystems (Tian et al. 2016; Spencer et al. 2017; Wu et al. 2018). An increasing awareness of coastal issues caused by

Received 22 May 2019. Accepted 19 March 2020.

L. Chen and J. Tao. State Key Laboratory of Hydrology-Water Resources and Hydraulic Engineering, Hohai University, Nanjing 210098, China; College of Harbor, Coastal and Offshore Engineering, Hohai University, Nanjing 210098, China.
Z. Zhou.* State Key Laboratory of Hydrology-Water Resources and Hydraulic Engineering, Hohai University, Nanjing 210098, China; Jiangsu Key Laboratory of Coast Ocean Resources Development and Environment Security, Hohai University, Nanjing 210098, China.
F. Xu. State Key Laboratory of Estuarine and Coastal Research, East China Normal University, Shanghai 200241, China.
M. Jimenez. Environmental Hydraulics Institute, "IH Cantabria", University of Cantabria, 39011 Santander, Spain.
C. Zhang. College of Harbor, Coastal and Offshore Engineering, Hohai University, Nanjing 210098, China.
Corresponding author: Zeng Zhou (email: zeng.zhou@hhu.edu.cn).
[1]This paper is part of a Collection entitled: In Search of Coastal Resilience (RCEM2017).
*Zeng Zhou currently serves as an Associate Editor; peer review and editorial decisions regarding this manuscript were handled by Ian Townend.

reduced intertidal areas has motivated the initiatives of de-reclamation (or restoration), aiming to return reclaimed land to the sea for a more rational and sustainable development of the coast (Gregory Hood 2004; Mekuria et al. 2011; Li et al. 2018).

Land reclamations have multiple impacts on the morphodynamics of tidal flats, and one of the most evident impacts is the cutting down of the drainage area of the tidal flow. Correspondingly, tidal prism and associated water flushing rates decrease, facilitating sediment deposition outside sea dikes (Flemming and Nyandwi 1994; Friedrichs 1995; Gao et al. 2014). With sediments continuously accreting after reclamation, intertidal flats tend to a new equilibrium state characterized by a gentle concave upper flat and a relatively steep convex lower flat (Wang et al. 2012). On the other hand, tidal level in front of sea dikes increases as a compensation for the decrease in drainage area. This may cause a higher risk in terms of dike stability (Song et al. 2013). By (partially) removing the dikes, de-reclamation projects have been conducted in a few countries to return reclaimed land to the sea. However, previous studies suggest that the hydrological regime, morphological status, and physical and chemical frameworks may not be fully restored. Spencer et al. (2017) found that the disturbance following restoration was evident for at least two decades and was likely to be irreversible. Many numerical models have been developed to analyze and predict the morphodynamic evolution after restoration. George et al. (2012) developed a numerical model to compare the historical changes of a restored estuary and predict its possible future morphological development. Yang et al. (2010) developed a three-dimensional numerical model to simulate the hydrodynamics after restoration, and model results combined with biological data showed that dike removal could result in desired conditions that support four habitat types (pond, tidal flat, low marsh, and high marsh) within the restoration footprint. In terms of field observation, Williams et al. (2002) collected extensive field data of restoration projects and found that tidal prism significantly increased after restoration and resulted in a further development of tidal channels. More specifically, these channels first deepened and then widened because of bank collapse.

Similar to reclamations, de-reclamation projects can also highly modify the morphology of tidal networks, which are common features in coastal areas. Tidal networks consist of multiple bifurcating and interweaving waterways, exerting a vital control on the ecomorphodynamics in coastal areas (Allen 2000; Friedrichs and Perry 2001; Coco et al. 2013; Kearney and Fagherazzi 2016). Tidal networks are primarily formed by tides, and they can be highly affected by waves and fluvial discharges. To understand the feedback mechanisms between the multiple processes and the morphology of tidal networks, a broad range of studies have been carried out, including field observations (Kleinhans et al. 2012; Vandenbruwaene et al. 2012; Jefferson and McGee 2013), laboratory experiments (Tambroni et al. 2005; Stefanon]et al. 2010, 2012; Vlaswinkel and Cantelli 2011), numerical simulations (D'Alpaos et al. 2005; Zhou et al. 2014*a*, 2014*b*; Xu et al. 2017), and theoretical derivations (Tarboton et al. 1988; Maritan et al. 1996; Rinaldo et al. 2004; Song et al. 2005). Among them, many studies have highlighted the control of the tidal basin geometry on the spatial patterns of tidal networks. For example, tidal networks in tidal lagoons show apple-tree shapes with sand barriers concentrating the flow in the inlet (Zhou et al. 2014*a*, 2014*b*), which is different from those developed on open-coast tidal flats (Belliard et al. 2015).

Notwithstanding, studies on the natural evolution of tidal networks have achieved great advances, but their development under the influence of land reclamations and de-reclamations has received less attention. These anthropogenic activities not only directly affect the hydrodynamic and sedimentary environments but also lead to considerable geomorphic reworking of topography in adjustment. In the present study, a state-of-the-art morphodynamic model (Delft3D) was employed to explore (*i*) the variations in tidal flow and sediment transport pattern and (*ii*) the long-term morphodynamic

evolution of tidal flat-channel systems in response to reclamation and de-reclamation projects. By addressing these objectives, this study aims to gain more insight into the role of these large-scale anthropogenic activities and hence provide a scientific basis for the protection and sustainable development of coastal resources. It is worth noting that this is a generalized numerical study aiming to provide insight into the physical indications of reclamation and de-reclamation projects in a qualitative rather than a quantitative manner.

2. Methods

An open-source morphodynamic model (Delft3D) was employed in this study (Lesser et al. 2004). Two-dimensional shallow water equations were solved for the tidal flow fields, which were utilized to calculate the sediment fluxes using the formula of Engelund and Hansen (1967). Then the bed level change was calculated through a bed continuity equation. Descriptions of these governing equations have been detailed in previous studies (Marciano et al. 2005; van der Wegen and Roelvink 2008; van Maanen et al. 2013; Zhou et al. 2014*a*, 2014*b*), and hence they are not reported here.

We considered a 25 km × 25 km rectangular computational domain (Fig. 1), of which the spatial grid resolution was 50 m × 50 m. The model geometry was composed of a flat region near the land with an initial random perturbation of ±15 cm (0 km < x < 12 km) and a linear slope toward the sea (12 km < x < 25 km). The initial bed elevation of the flat region was set to mean sea level (MSL) and the slope of the seaside lower part was 1‰. The initial bathymetry was perturbed to accelerate the onset of the morphodynamic evolution. The seaward boundary (i.e., $x = 25$ km) was forced by the M_2 tidal constituent with an amplitude of $a = 2.4$ m. All the other three boundaries were closed to allow the tidal wave to perpendicularly enter the tidal basin. The characteristic grain size of the sediment was $D_{50} = 200$ μm. An "equilibrium boundary condition" technique was used so that the sediment flux passing through the seaward boundary was calculated based on the local flow conditions to ensure that the change of the bed level at the boundary was minimal (van der Wegen and Roelvink 2008). To reduce the simulating time of long-term morphological models, the bed level changes at each time step were scaled up linearly by a morphological factor following the approach of Roelvink (2006).

To analyze the morphodynamic evolution of tidal networks in response to reclamation and de-reclamation projects, a three-stage simulation was designed. In the first stage, the natural development of tidal networks was modelled without anthropogenic interventions. At the beginning of the second stage, parts of the computational domain were enclosed by sea dikes, which represented the implementation of the reclamation project. Two sea dike arrangement options were studied: the landward portion was (*i*) partly enclosed (0 km < x < 10 km, 4 km < y < 14 km) or (*ii*) fully enclosed (0 km < x < 10 km, 0 km < y < 18 km). These sea dikes were removed or opened in the third stage to simulate the recovery of the tidal networks after de-reclamation. Each stage lasted for 100 years (i.e., 300 years in total), which allowed adequate time for the morphodynamic evolution of the tidal networks. Combinations of the different options in the second and third stages lead to the four numerical experiments as listed in Table 1 (Run 2–Run 5). An additional run, denoted as Run 1, without anthropogenic interventions throughout the simulation was performed for comparison.

Other common parameters used with standard values in this study included the time step ($t = 0.5$ min), Chézy coefficient ($C = 65$ m$^{1/2}$/s), horizontal eddy viscosity ($\nu = 1$ m^2/s), and morphological scale factor (MorFac = 50).

Fig. 1. (*a*) Initial bathymetry of the model with respect to mean sea level, and (*b*) profile shape of the location indicated by the dashed line in subplot (*a*).

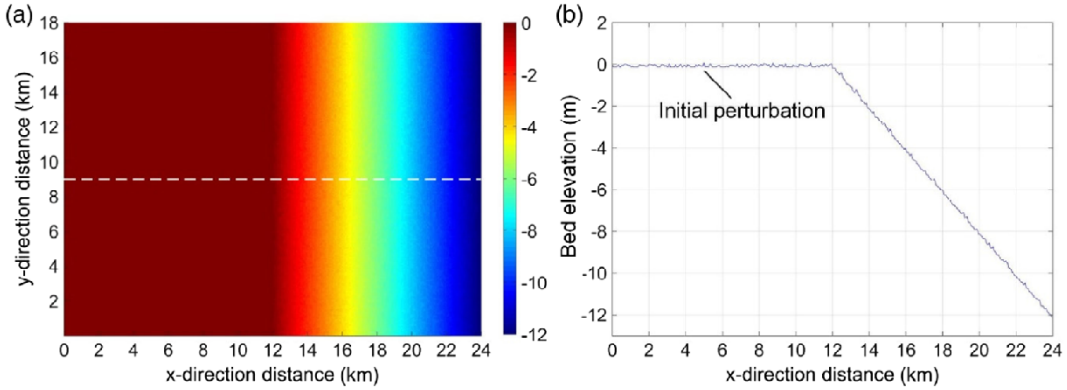

Table 1. Design of numerical experiments with reclamation and de-reclamation.

Runs	Stage 1: Year 0–100	Stage 2: Year 100–200 reclamation	Stage 3: Year 200–300 de-reclamation
Run 1	Naturally evolved		
Run 2	Naturally evolved	Partly enclosed	Removed
Run 3	Naturally evolved	Partly enclosed	Opened
Run 4	Naturally evolved	Fully enclosed	Removed
Run 5	Naturally evolved	Fully enclosed	Opened

3. Results and discussion

3.1. Natural development of tidal networks

In the first 100 years, tidal networks developed rapidly from an initially flat bed to a complex channel-flat system, covering the vast majority of the upper flat region. A rough division of the primary and secondary tidal channels was observed at the cross-shore distance of approximately 12 km (Fig. 2*a*). The distribution of tidal channels was relatively uniform in the along-shore direction, since the boundary conditions and the model geometry were almost uniform except for some imposed initial bathymetrical perturbations. Comparable to natural tidal channel networks, extensive channel branches were formed in the landward portion with a meandering characteristic. Delta-shaped features were formed in the seaward portion, which implies a net sediment flux in the ebb direction. With time (e.g., after 200 years), the structure of tidal networks became asymptotically stable in the landward portion, while continuously extending in the seaward direction with channel deepening (Figs. 2*b* and 2*c*). We chose the resultant morphologies after 100 and 200 years for the implementation of the reclamation and de-reclamation projects in Run 2–Run 5.

A close scrutiny of the local detailed morphological evolution was carried out by monitoring three representative transects along the cross-shore direction (indicated by C1, C2, and C3 in Fig. 2*a*). Cross-section C1 was near the land boundary ($x = 3$ km) with relatively weaker tidal hydrodynamics, so the channels developed there were of small depths and widths, which increased slightly over time (Fig. 2*d*). Cross-section C2 was located in the transitional region between the initial flat platform and the slope. Because of the relatively large change in elevation (favoring a larger flow velocity), tidal channels formed more rapidly near C2 (Fig. 2*g*), and they tended to be wider and deeper than the channels near

Fig. 2. Naturally evolved morphology of Run 1: (*a*) Resultant morphology after 100 years, (*b*) after 200 years, and (*c*) after 300 years. The color scheme indicates the bed elevation (m) with respect to mean sea level. (*d*, *e*, *and f*) Cross-sections of C1, C2, and C3, respectively, indicated in subplot (*a*). (*g*) Evolution of the number of tidal channels per kilometer.

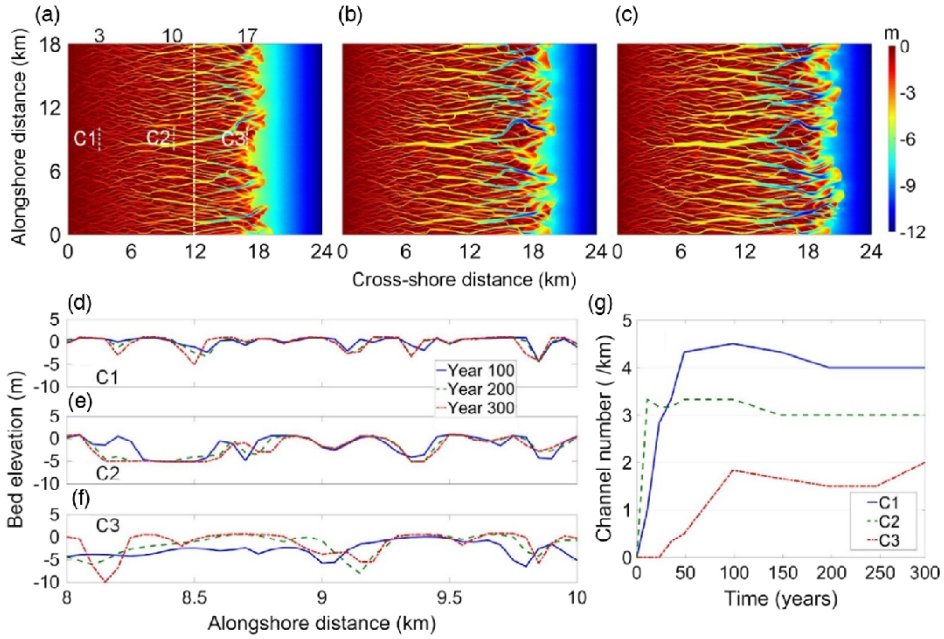

C1 (Fig. 2*e*). Within the first 100 years, the channels developed at both C1 and C2 showed a pronounced change in cross-sectional shape, while they approached relatively stable configurations after 200 years with only minor local modifications. The numbers of channels per kilometer were about 4 and 3 for C1 and C2, respectively, indicating weak branching behavior (Fig. 2*g*). Tidal channels start to form near cross-section C3 after about 100 years (later than that near C1 and C2) because of the gradual process of sediment erosion in the flat platform. The eroded sediment was transported seaward and accumulated to a certain elevation that favors the formation of tidal channels. Because of stronger tidal current, the channels near C3 were larger with a maximum depth of up to 10 m (Fig. 2*f*).

3.2. Effect of land reclamation

Figure 3 shows the spatial patterns of the tidal network morphologies as well as the bed level changes 100 years after the construction of sea dikes for both the fully and partly enclosed cases (i.e., year 200). The morphodynamic evolution in the enclosed areas was terminated, since the movements of flow and sediment were cut off. Moreover, the morphodynamic evolution was limited in front of the sea dikes, which straightly obstructs perpendicular incident flow. For the partly enclosed case, the cross-sectional area experienced a sudden decrease in the upstream direction, which resulted in the convergence and divergence of the flood and ebb tidal flow. Therefore, the tidal channels adjacent to the corner bend in response. Moreover, the concentration of tidal flow promotes the development of tidal networks in the upper flat flanking the enclosed area.

Figure 4 compares the residual tidal currents around the sea dikes between the natural and partly enclosed cases. Three typical areas were investigated, focusing on the corner (Area 1), the front sea dike (Area 2), and the lower flat (Area 3). The fully enclosed case is

Fig. 3. (*a*) Resultant morphology of the partly enclosed reclamation after 200 years. (*b*) Morphological difference in "erosion–deposition" patterns between the partly enclosed reclamation case and the naturally evolved case after 100 years. (*c*) Resultant morphology of the fully enclosed reclamation after 200 years. (*d*) Difference in "erosion–deposition" patterns between the fully enclosed reclamation case and the naturally evolved case after 100 years. The color scheme indicates the bed elevation (m). The selected locations of Area 1, Area 2, and Area 3, which are considered for further analyses, cover areas of ($x = 9$–13 km, $y = 12$–16 km), ($x = 9$–13 km, $y = 7$–11 km), and ($x = 14$–18 km, $y = 7$–11 km), respectively.

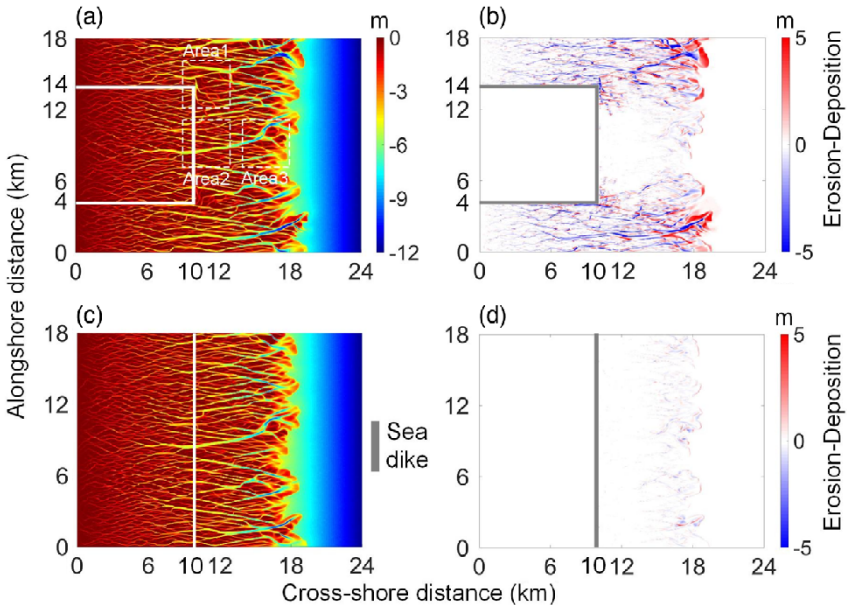

not shown, since the variations are similar to those of Area 2 and Area 3 of the partly enclosed case. For Area 1, the residual tidal current velocities in channels at the side only decreased in magnitude, while at the corner, their directions turned to the adjacent flats, where the residual tidal currents deflect and diverge (Fig. 4*a*). In Area 2, the velocities are small (Fig. 4*b*) even in the channels, which resulted in tiny morphological variation. Moreover, the direction of the residual currents on the ridges were changed from landward to seaward after the reclamation. Although the decrease in velocities and changes in directions still occur in Area 3, the influences were weaker with the increase of distance from the sea dike (Fig. 4*c*).

Figure 5 shows the mean bed elevation change of the upper flat area throughout the 300-year simulation. The morphodynamic evolution of the enclosed cases was limited to between years 100 and 200, which can be attributed to the reduced sediment source eroded from the upper intertidal area, as well as a reduced tidal prism resulting from reclamation projects. The fully enclosed reclamation case resulted in less bed level changes than that of the partly enclosed case. The reason is that the seaside region (10 km $< x <$ 24 km) in the partly enclosed case can still receive sediment from the upper tidal flat, while the fully enclosed case does not. In the partly enclosed case, erosion occurred from about 2 km across the shore (Fig. 6*a*) and became strengthened seaward (i.e., from 7 to 11 km, Fig. 6*b*), indicating a sediment export from the upper tidal flat toward the sea. The sediment sink was at the seaward end of channels (i.e., from 16 to 20 km, Fig. 6*c*). However, in the fully enclosed case, only a tiny bed elevation change occured in front of the dike (Figs. 6*d*–6*f*) because no sediment source eroded from the upper tidal flat. This highlights the effects of

Fig. 4. Residual current and morphology in (*a*) Area 1, (*b*) Area 2, and (*c*) Area 3 after 100 years. The arrows represent residual currents within the no reclamation and partly enclosed cases. The color scheme indicates the bed elevation (m).

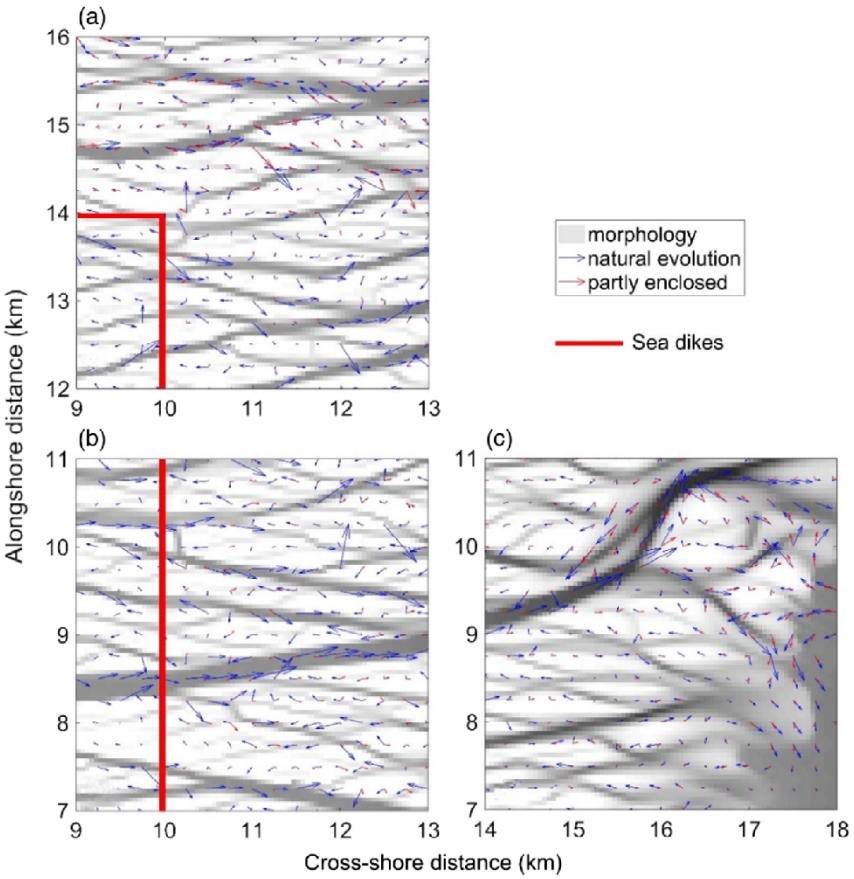

the sediment sources from the upper tidal flat to the formation of the tidal networks in the seaward portion.

Model results under the reclamations are in line with the measured data along the Jiangsu Coast, China, as demonstrated in Zhang et al. (2013) who also found that erosion was pronounced around the corner of the project area and the effect of the reclamation project on morphodynamic processes was only concentrated near the project area.

3.3. Effect of the de-reclamation

Based on previous reclamation schemes, several de-reclamation schemes were explored by breaching or removing the seawalls. Before the de-reclamations, the bed elevation was reset in the reclaimed area to 0 m to mimic human intervention. As a comparison, a no-reset case was considered in which the previously reclaimed channel–shoal morphology is not changed. When removing all the sea dikes, although the previously reclaimed areas are returned, the morphology cannot be fully restored to its original natural state (Fig. 7). De-reclamations tend to induce landward sediment transport so that tidal channels continuously develop and extend in the seaward direction.

First considered was the de-reclamation schemes of removing all dikes (removing-all) (Figs. 7*a* and 7*d*). For the partly enclosed case, the morphodynamic evolution of tidal

Fig. 5. Mean bed elevation change in a region of 14 km × 18 km, whose cross-shore distance is 10–24 km and along-shore distance is 0–18 km.

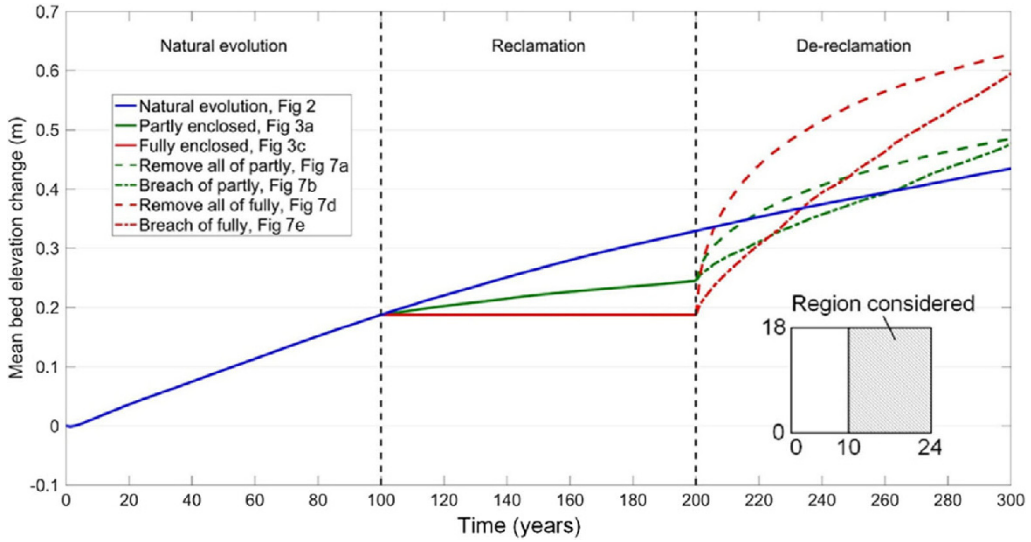

Fig. 6. Cross-shore distribution of bed elevation change (along-shore averaged) from years 100 to 200. (*a*) The partly enclosed reclamation case: (*b*) eroded part and (*c*) deposited part. (*d*) The fully enclosed reclamation case: (*e*) eroded part and (*f*) deposited part. The arrows indicate the trend of bed elevation change with time.

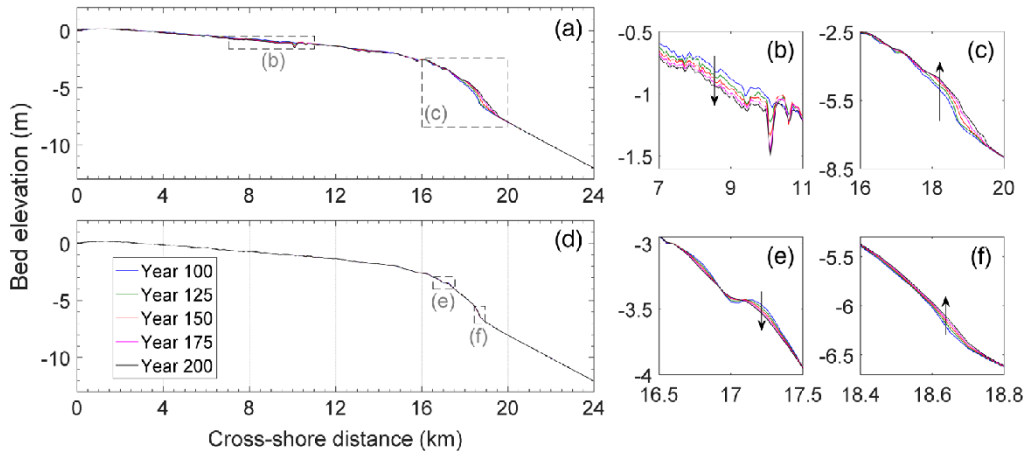

channels after de-reclamation near the restored area was more intense than the channels in front of the dikes. Tidal channels cut into the reset reclaimed flat area from three sides, and thus the restored morphology displayed a radial pattern (Fig. 7*a*). The channels outside the reclaimed area before de-reclamations, which turn direction at the corner of the dikes, were deepened and also branched into smaller channels towards the restored area. For the fully enclosed case, the channels outside the reclaimed area cut into the reclaimed flat region after removing all dikes (Fig. 7*d*). Branching behaviors of tidal channels were observed toward the landward portion of the tidal flat. Noticeably, there was an obvious depth difference of the tidal channels at the original dike location after de-reclamation

Fig. 7. (*a*–*c*) Simulated morphologies after de-reclamation based on the partly enclosed reclamation case: (*a*) removing all dikes, (*b*) opening breaches with resetting the reclaimed area to a bed level of 0 m, and (*c*) removing all dikes without resetting the bed level to 0 m in the reclamation area. (*d*–*e*) Simulated morphologies after de-reclamation based on the fully enclosed reclamation case: (*d*) removing all dikes and (*e*) opening breaches with resetting the reclaimed area to a bed level of 0 m. The results of all cases are after 300 years. White solid lines indicate sea dikes and white dotted lines indicate removed dikes. (*f*) Boxes B1, B2, and B3 show some of the local morphologies in detail.

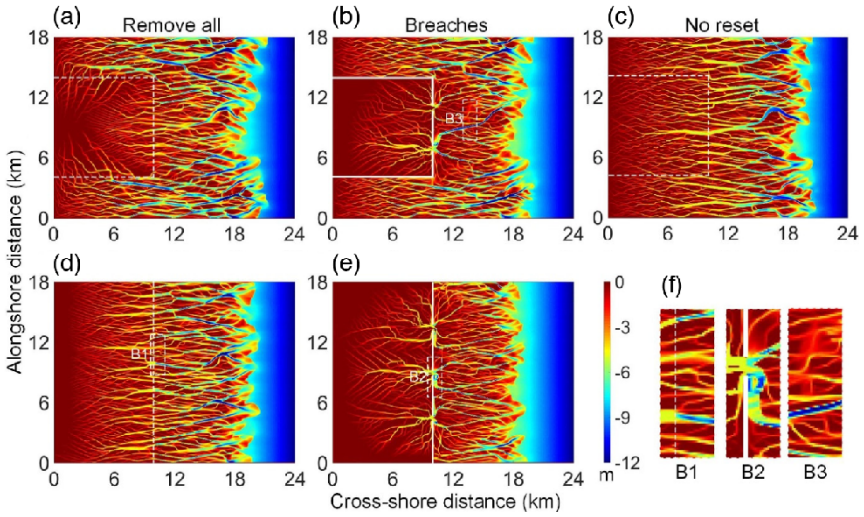

(see B1 in Fig. 7*f*). Because of the weaker tidal hydrodynamics, the newly developed channels in the restored area were much shallower than the outside ones cut by the original dike. This result is more similar to the natural case, rather than the reset case. Because less evolution occurred in front of the dike, channels there easily connected with the channels in the project area, which was similar to before the project, and even the channels at corners were restored.

Next considered was the de-reclamation schemes of opening breaches (opening-breach) (Figs. 7*b* and 7*e*). Breaches in sea dikes can significantly change the local tidal hydrodynamics because the breaches can concentrate the flow entering the reclaimed area, which work similarly to the sand barriers in coastal lagoons. Correspondingly, the channels near the breaches were deepened (B2 in Fig. 7*f*), while those far from breaches branched into tributary channels. In front of the dike, only the main channels presented significant deepening (B3 in Fig. 7*f*), while variations in the widths and depths of other channels in front of the dike were minor. The overall development of tidal channels in the opening-breach case was slower than that of the removing-all case. However, deeper tidal channels can form in the opening-breach case because of the concentration of tidal flow.

In the beginning, the increase in mean bed elevation of the removing-all case was more evident than that of the opening-breach case (Fig. 5). However, the increase then slowed down in the removing-all case, while in the opening-breach case it kept increasing at a steady rate owing to the constrained entrances of breaches (Fig. 5). In terms of the fully enclosed case, the tendency of the bed elevation change was comparable to the partly enclosed case. These results indicate that removing all dikes tends to cause a more dramatic influence on tidal channel-flat morphology at the beginning, while opening breaches may have a longer influence.

Fig. 8. Evolution of the mean unchannelled flow length with time. The region considered is the entire simulating area.

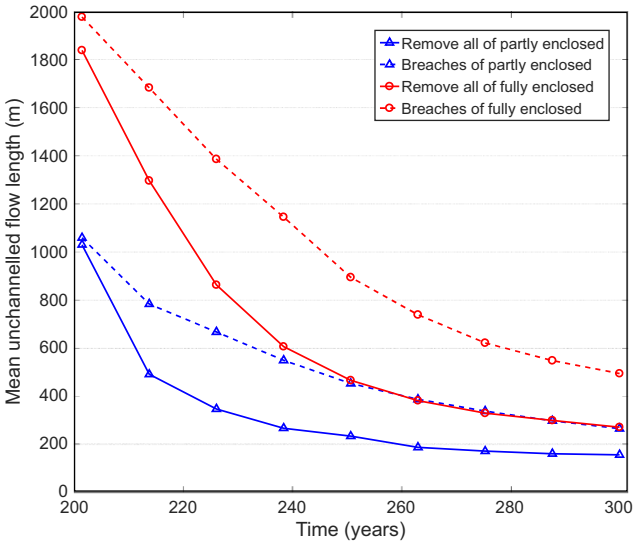

Drainage density is an important parameter for understanding channel network systems (Moglen et al. 1998; Zhou et al. 2014*a*, 2014*b*). The mean unchanneled flow length (l_m) was used to represent drainage density, as proposed by Marani et al. (2003), and is defined as the mean distance from a point on the platform to the closest channel. At the beginning, the value of l_m was large because the project area was reset at that time, but then it decreased rapidly during tidal network development and finally slowed down (Fig. 8). The decreasing value of l_m was faster for the removing-all case than for the opening-breach case, and its final value was smaller because when remove all dikes the channels developed much faster. The results also showed that the drainage density of the removing-all case was larger than the opening-breach case, which suggests that the channel networks were more efficient in draining tidal flats when all dikes were removed and also indicates that there was a more rapid development of the tidal networks.

3.4. Implications for coastal management and further study

Coastal reclamation is a common anthropogenic activity to gain valuable land resources; however, there is an increasing awareness of its irreversible side effects. Model results of this study indicate that land reclamations can greatly affect the morphodynamics near sea dikes over shorter time scales (e.g., months to years). Tidal channels far from the dikes may not be influenced significantly by reclamation over shorter time scales, but the influence can gradually accumulate and become evident over longer time scales (e.g., tens of years). Therefore, both short-term and long-term morphological responses after land reclamation should be carefully examined before reclamation projects are implemented. Tidal channel evolution can be considerably modified by the construction of sea dikes. For instance, tidal channels in front of sea dikes (especially those at the corners) tend to grow along the dikes, which poses a threat to the stability of the dikes.

De-reclamations or restorations have become increasingly popular over the last decades under the consideration of coastal protection and ecological and environmental issues. When sea dikes are breached or fully removed, the morphology of the restored area changes dramatically. Tidal channels can cut through the restored area and greatly enhance

the exchange of water and nutrients, which is beneficial to wetland restoration. Model results show that different de-reclamation schemes have different morphological impacts. For example, opening breaches can significantly modify the spatial distribution of channels near the breach, leading to considerable local morphological change. Moreover, the case without resetting the bed level to 0 m (Fig. 7*c*) showed a more natural result than the case of resetting the level (Fig. 7*a*), which may provide an idea that if we want to restore the projected area to its natural state, we can make some suitable artificial channels inside the area in advance.

In the present study, only tides were considered in shaping the morphology of tidal networks. However, there is still a lack of sound and integrated physical descriptions for several processes operating on intertidal flats. For instance, de-reclamations mainly serve to protect and improve coastal habitats and biological resources (Yang et al. 2010), and thus, how the vegetation develops under the influence of anthropogenic activities is an important issue. Meanwhile, a significant feature of vegetation is capturing sediment particles and accumulation (Mudd et al. 2010), so multiple sediments should be considered (e.g., mud and sand). Moreover, waves are not accounted for, where they may enhance the suspension of surficial sediment on tidal flats, which may also play an important role in intertidal morphodynamics with anthropogenic activities.

4. Conclusions

A state-of-the-art numerical model (Delft3D) was used to explore the morphodynamics of tidal networks under the influence of reclamation and de-reclamation projects. Model results indicated that reclamation projects can alter the residual current distribution in tidal flat-channel systems and hence affect the development of tidal networks. Meanwhile, the influence of dikes showed a spatial variation. For the partly enclosed case, channels barely developed in front of the dikes because of the lack of both sediment source and strong hydrodynamic force, while tidal networks kept developing in the upper flat flanking the enclosed area. Moreover, channels near the corners of the dikes diverted because of the convergence and divergence of the tidal flow. For the fully enclosed case, because of the uniformity in the along-shore direction, the results were similar to the area in front of the dikes in the partly enclosed case. The affected region of reclamation was limited to the area surrounding the dikes.

De-reclamation projects promote or alter the evolution of the channel system, depending on the methods of de-reclamation (i.e., removing all dikes or opening breaches). The method of removing all dikes restored the hydrodynamic environment of the tidal flat similar to the original situation, but the morphology cannot be fully restored. In this study, we considered two initial settings for the reclaimed area: (*i*) resetting the bed elevation in the reclaimed area to 0 m and (*ii*) keeping the bed as it is without any change. The results indicate that the latter setting leads to a more natural morphology. Moreover, the channels outside the restored area were deeper than the inner ones. As for the case of opening breaches, the flow was constrained in the entrances leading to a tree-like network structure. The channels near the breaches and the main channels in front of the dikes were deepened, while the channels further away from the breaches branched into tributary channels. By comparing these two de-reclamation methods, it appears that removing all dikes tends to cause a more dramatic influence on tidal channel-flat morphology in the beginning, whereas opening breaches may have a longer influence. Moreover, the channel networks were more efficient in draining tidal flats when all dikes were removed.

Acknowledgements

This study is supported by the National Natural Science Foundation of China (NSFC, Grant Nos. 41976156 and 51620105005) and the Jiangsu Marine Science and Technology Innovation Programme (Grant No. HY2018-1).

References

Allen, J.R.L. 2000. Morphodynamics of Holocene salt marshes: A review sketch from the Atlantic and Southern North Sea coasts of Europe. Quat. Sci. Rev. **19**(12): 1155–1231. doi:10.1016/S0277-3791(99)00034-7.

Belliard, J.-P., Toffolon, M., Carniello, L., and D'Alpaos, A. 2015. An ecogeomorphic model of tidal channel initiation and elaboration in progressive marsh accretional contexts. J. Geophys. Res.: Earth Surf. **120**(6): 1040–1064. doi:10.1002/2015JF003445.

Coco, G., Zhou, Z., van Maanen, B., Olabarrieta, M., Tinoco, R., and Townend, I. 2013. Morphodynamics of tidal networks: Advances and challenges. Mar. Geol. **346**: 1–16. doi:10.1016/j.margeo.2013.08.005.

D'Alpaos, A., Lanzoni, S., Marani, M., Fagherazzi, S., and Rinaldo, A. 2005. Tidal network ontogeny: Channel initiation and early development. J. Geophys. Res.: Earth Surf. **110**(F2): F02001. doi:10.1029/2004JF000182.

Engelund, F., and Hansen, E. 1967. A monograph on sediment transport in alluvial streams. Vol. 33. Teknisk Forlag, Copenhagen, Denmark. 62 pp.

Flemming, B.W., and Nyandwi, N. 1994. Land reclamation as a cause of fine-grained sediment depletion in backbarrier tidal flats (Southern North Sea). Neth. J. Aquat. Ecol. **28**(3–4): 299–307. doi:10.1007/BF02334198.

Friedrichs, C.T. 1995. Stability shear stress and equilibrium cross-sectional geometry of sheltered tidal channels. J. Coastal Res. **11**(4): 1062–1074.

Friedrichs, C.T., and Perry, J.E. 2001. Tidal salt marsh morphodynamics: A synthesis. J. Coastal Res. **SI27**: 7–37.

Gao, G.D., Wang, X.H., and Bao, X.W. 2014. Land reclamation and its impact on tidal dynamics in Jiaozhou Bay, Qingdao, China. Estuarine, Coastal Shelf Sci. **151**: 285–294. doi:10.1016/j.ecss.2014.07.017.

George, D.A., Gelfenbaum, G., and Stevens, A.W. 2012. Modeling the hydrodynamic and morphologic response of an estuary restoration. Estuaries Coasts, **35**(6): 1510–1529. doi:10.1007/s12237-012-9541-8.

Gregory Hood, W. 2004. Indirect environmental effects of dikes on estuarine tidal channels: Thinking outside of the dike for habitat restoration and monitoring. Estuaries, **27**(2): 273–282. doi:10.1007/BF02803384.

Jefferson, A.J., and McGee, R.W. 2013. Channel network extent in the context of historical land use, flow generation processes, and landscape evolution in the North Carolina Piedmont. Earth Surf. Processes Landforms, **38**(6): 601–613. doi:10.1002/esp.3308.

Kearney, W.S., and Fagherazzi, S. 2016. Salt marsh vegetation promotes efficient tidal channel networks. Nat. Commun. **7**: 12287. doi:10.1038/ncomms12287. PMID:27430165.

Kleinhans, M.G., van der Vegt, M., van Scheltinga, R.T., Baar, A.W., and Markies, H. 2012. Turning the tide: Experimental creation of tidal channel networks and ebb deltas. Neth. J. Geosci. **91**(3): 311–323. doi:10.1017/S0016774600000469.

Lesser, G.R., Roelvink, J.A., van Kester, J.A.T.M., and Stelling, G.S. 2004. Development and validation of a three-dimensional morphological model. Coastal Eng. **51**(8–9): 883–915. doi:10.1016/j.coastaleng.2004.07.014.

Li, X., Bellerby, R., Craft, C., and Widney, S.E. 2018. Coastal wetland loss, consequences, and challenges for restoration. Anthropocene Coasts, **1**(1): 1–15. doi:10.1139/anc-2017-0001.

Lotze, H.K., Lenihan, H.S., Bourque, B.J., Bradbury, R.H., Cooke, R.G., Kay, M.C., et al. 2006. Depletion, degradation, and recovery potential of estuaries and coastal seas. Science, **312**(5781): 1806–1809. doi:10.1126/science.1128035. PMID:16794081.

Marani, M., Belluco, E., D'Alpaos, A., Defina, A., Lanzoni, S., and Rinaldo, A. 2003. On the drainage density of tidal networks. Water Resour. Res. **39**(2): 1040. doi:10.1029/2001WR001051.

Marciano, R., Wang, Z.B., Hibma, A., de Vriend, H.J., and Defina, A. 2005. Modeling of channel patterns in short tidal basins. J. Geophys. Res.: Earth Surf. **110**(F1): F01001. doi:10.1029/2003JF000092.

Maritan, A., Colaiori, F., Flammini, A., Cieplak, M., and Banavar, J.R. 1996. Universality classes of optimal channel networks. Science, **272**: 984–986. doi:10.1126/science.272.5264.984. PMID:8662583.

Mekuria, W., Veldkamp, E., Tilahun, M., and Olschewski, R. 2011. Economic valuation of land restoration: The case of exclosures established on communal grazing lands in Tigray, Ethiopia. Land Degrad. Dev. **22**(3): 334–344. doi:10.1002/ldr.1001.

Moglen, G.E., Eltahir, E.A.B., and Bras, R.L. 1998. On the sensitivity of drainage density to climate change. Water Resour. Res. **34**(4): 855–862. doi:10.1029/97WR02709.

Mudd, S.M., D'Alpaos, A., and Morris, J.T. 2010. How does vegetation affect sedimentation on tidal marshes? Investigating particle capture and hydrodynamic controls on biologically mediated sedimentation. J. Geophys. Res.: Earth Surf. **115**(F3): F03029. doi:10.1029/2009JF001566.

Portnoy, J.W., and Giblin, A.E. 1997. Effects of historic tidal restrictions on salt marsh sediment chemistry. Biogeochemistry, **36**(3): 275–303. doi:10.1023/A:1005715520988.

Rinaldo, A., Belluco, E., D'Alpaos, A., Feola, A., Lanzoni, S., and Marani, M. 2004. Tidal networks: Form and function. *In* The ecogeomorphology of tidal marshes. *Edited by* S. Fagherazzi, M. Marani, and L.K. Blum. AGU, Washington, D.C., USA. pp. 75–91.

Roelvink, J.A. 2006. Coastal morphodynamic evolution techniques. Coastal Eng. **53**(2–3): 277–287. doi:10.1016/j.coastaleng.2005.10.015.

Song, C., Havlin, S., and Makse, H.A. 2005. Self-similarity of complex networks. Nature, **433**(7024): 392–395. doi:10.1038/nature03248. PMID:15674285.
Song, D., Wang, X.H., Zhu, X., and Bao, X. 2013. Modeling studies of the far-field effects of tidal flat reclamation on tidal dynamics in the East China Seas. Estuarine, Coastal Shelf Sci. **133**: 147–160. doi:10.1016/j.ecss.2013.08.023.
Spencer, K.L., Carr, S.J., Diggens, L.M., Tempest, J.A., Morris, M.A., and Harvey, G.L. 2017. The impact of pre-restoration land-use and disturbance on sediment structure, hydrology and the sediment geochemical environment in restored saltmarshes. Sci. Total Environ. **587**–**588**: 47–58. doi:10.1016/j.scitotenv.2016.11.032. PMID:28215810.
Stefanon, L., Carniello, L., D'Alpaos, A., and Lanzoni, S. 2010. Experimental analysis of tidal network growth and development. Cont. Shelf Res. **30**(8): 950–962. doi:10.1016/j.csr.2009.08.018.
Stefanon, L., Carniello, L., D'Alpaos, A., and Rinaldo, A. 2012. Signatures of sea level changes on tidal geomorphology: Experiments on network incision and retreat. Geophys. Res. Lett. **39**(12): L12402. doi:10.1029/2012GL051953.
Tambroni, N., Bolla Pittaluga, M., and Seminara, G. 2005. Laboratory observations of the morphodynamic evolution of tidal channels and tidal inlets. J. Geophys. Res.: Earth Surf. **110**(F4): F04009. doi:10.1029/2004JF000243.
Tarboton, D.G., Bras, R.L., and Rodriguez-Iturbe, I. 1988. The fractal nature of river networks. Water Resour. Res. **24**(8): 1317–1322. doi:10.1029/WR024i008p01317.
Tian, B., Wu, W., Yang, Z., and Zhou, Y. 2016. Drivers, trends, and potential impacts of long-term coastal reclamation in China from 1985 to 2010. Estuarine, Coastal Shelf Sci. **170**: 83–90. doi:10.1016/j.ecss.2016.01.006.
van der Wegen, M., and Roelvink, J.A. 2008. Long-term morphodynamic evolution of a tidal embayment using a two-dimensional, process-based model. J. Geophys. Res.: Oceans, **113**(C3): C03016. doi:10.1029/2006JC003983.
van Maanen, B., Coco, G., and Bryan, K.R. 2013. Modelling the effects of tidal range and initial bathymetry on the morphological evolution of tidal embayments. Geomorphology, **191**: 23–34. doi:10.1016/j.geomorph.2013.02.023.
Vandenbruwaene, W., Meire, P., and Temmerman, S. 2012. Formation and evolution of a tidal channel network within a constructed tidal marsh. Geomorphology, **151**–**152**: 114–125. doi:10.1016/j.geomorph.2012.01.022.
Vlaswinkel, B.M., and Cantelli, A. 2011. Geometric characteristics and evolution of a tidal channel network in experimental setting. Earth Surf. Processes Landforms, **36**(6): 739–752. doi:10.1002/esp.2099.
Wang, Y.P., Gao, S., Jia, J., Thompson, C.E.L., Gao, J., and Yang, Y. 2012. Sediment transport over an accretional intertidal flat with influences of reclamation, Jiangsu coast, China. Mar. Geol. **291**–**294**: 147–161. doi:10.1016/j.margeo.2011.01.004.
Williams, P.B., Orr, M.K., and Garrity, N.J. 2002. Hydraulic geometry: A geomorphic design tool for tidal marsh channel evolution in wetland restoration projects. Restor. Ecol. **10**(3): 577–590. doi:10.1046/j.1526-100X.2002.t01-1-02035.x.
Wu, W., Yang, Z., Tian, B., Huang, Y., Zhou, Y., and Zhang, T. 2018. Impacts of coastal reclamation on wetlands: Loss, resilience, and sustainable management. Estuarine, Coastal Shelf Sci. **210**: 153–161. doi:10.1016/j.ecss.2018.06.013.
Xu, F., Coco, G., Zhou, Z., Tao, J., and Zhang, C. 2017. A numerical study of equilibrium states in tidal network morphodynamics. Ocean Dyn. **67**(12): 1593–1607. doi:10.1007/s10236-017-1101-0.
Yang, Z., Sobocinski, K.L., Heatwole, D., Khangaonkar, T., Thom, R., and Fuller, R. 2010. Hydrodynamic and ecological assessment of nearshore restoration: A modeling study. Ecol. Modell. **221**(7): 1043–1053. doi:10.1016/j.ecolmodel.2009.07.011.
Zhang, C., Zheng, J., Dong, X., Cao, K., and Zhang, J. 2013. Morphodynamic response of Xiaomiaohong tidal channel to a coastal reclamation project in Jiangsu Coast, China. J. Coastal Res. **65**: 630–635. doi:10.2112/SI65-107.1.
Zhou, Z., Olabarrieta, M., Stefanon, L., D'Alpaos, A., Carniello, L., and Coco, G. 2014*a*. A comparative study of physical and numerical modeling of tidal network ontogeny. J. Geophys. Res.: Earth Surf. **119**(4): 892–912. doi:10.1002/2014JF003092.
Zhou, Z., Stefanon, L., Olabarrieta, M., D'Alpaos, A., Carniello, L., and Coco, G. 2014*b*. Analysis of the drainage density of experimental and modelled tidal networks. Earth Surf. Dyn. **2**(1): 105–116. doi:10.5194/esurf-2-105-2014.